IMPACT OF IN-LINE CLEAR-SKY SIMULATIONS EXPECTED FOR THE NWCSAF GEO CLOUD MASK

Marcel Derrien, Hervé Le Gléau, Marie-Paule Raoul

Météo-France / DP / Centre de Météorologie Spatiale. BP 50747. 22307 Lannion. France

Abstract

SAFNWC (http://nwcsaf.org) consortium has developed a software package to extract various products from MSG/SEVIRI imagery. The first version of this software package has been made available to users in June 2004. Next major milestone of the project is the delivery of V2015 release of the GEO software package. Its design is improved to include new products and is technically adapted to process foreign geostationary satellites. Moreover it is prepared for the processing of next generation of Meteosat MTG.
Meteo-France has developed the part of the software package dedicated to the cloud products retrieval (cloud mask and types, cloud top temperature and height) from MSG SEVIRI imagery. This poster summarizes and illustrates the expected cloud mask improvements as observed during a prototyping activity and to be implemented in V2015

BACKGROUND

The Satellite Application Facility in support to Nowcasting (SAFNWC) is part of EUMETSAT ground segment. It provides targeted users with software packages for the generation of satellite-derived products useful for nowcasting purposes. One package is designed specifically for data on board polar platform satellites (NOAA and METOP) and the other one for the data of geostationary satellite Meteosat Second Generation (MSG).
The first version of this software package has been made available to users in June 2004 (Derrien et al., 2005). Since then, regular versions are released which include scientific and technical improvements implemented according to user's requirements inventoried during regular workshops (Derrien et al., 2010).
The current version of the NWCSAF cloud mask algorithm for infrared thresholds is based on pre-calculated look-up tables derived from off-line radiative transfer simulations and depending on atlas, illumination conditions, integrated water vapour content from Numerical Weather Prediction (NWP) models, viewing angle and forecasted surface temperature. The use of in-line clear-sky simulations is already implemented in operational schemes (Lutz 2008, Heidinger 2011, Hocking 2011). In our context its aim is to capture clouds missed by the current operational cloud mask (particularly at night) without adding false alarms. This paper summarizes and illustrates the cloud mask improvements based on the use of in-line clear-sky simulations to be implemented in the SAFNWC/MSG SW V2015.

CLEAR-SKY SIMULATIONS PRINCIPLE

The clear-sky radiance is the sum of three contributions: the surface emission, the upwelling atmosphere emission, and the reflexion of the downwelling atmosphere emission by the surface, when the reflected solar radiation can be ignored (not the case for 3.9μm at daytime).

$$R = \varepsilon_s(\nu,\theta)B(\nu,Ts)\tau_s(\nu,\theta) + \int_{\tau_s}^{1} B(\nu,T)d\tau + (1-\varepsilon_s(\nu,\theta))\tau_s^2 \int_{\tau_s}^{1} B(\nu,T)\frac{B(\nu,T)}{\tau^2}d\tau \quad (1)$$

τ_s is the surface to space transmittance, ε_s is the surface emissivity, B(ν,T) in the Planck function at temperature T for wave number ν. These terms can be split into pieces that are atmosphere and

surface related. The atmospheric state is derived from ECMWF forecasted fields with 91 levels (137 since June 2013) with a 3h temporal step. We assume that the surface emissivity is constant for sea, and for land we rely on the emissivity atlas embedded in RTTOV10 providing monthly values. Therefore we can interpolate in time, the transmittance, the atmospheric emission, and the downward term. The local radiance can then be derived using equation 1 with the local emissivity derived from atlas and an adaptation of the NWP skin temperature to the local topography over land, and over ocean the SST from OSTIA (Stark et al.,2007) (preferred to NWP skin temperature for its better spatial resolution). OSTIA produces a foundation SST estimate (free of diurnal cycle) at an input grid of 1/20°, it is converted to a skin SST by subtracting 0.2K. This analysed temperature is produced daily and can be used operationally as soon as available for users. Over land, in order to have a better description of atmosphere and surface a high spatial resolution of NWP is desirable.

EXAMPLES

Improving detection of low clouds over sea in night-time

The sharpest histogram of the differences between clear SEVIRI observations and their simulations (Figure 1) reveals that the 3.9μm simulations should be the best tool for the detection of the remaining clouds after the operational cloud mask. Therefore we rely mainly on 3.9μm simulations to improve the cloud detection over sea in night-time.

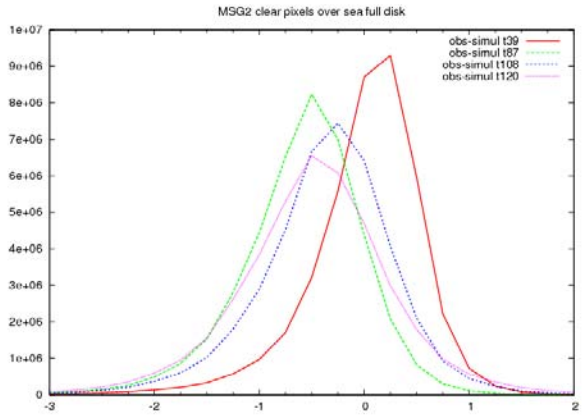

Figure 1 : **Histogram of observed minus simulated Meteosat-9 SEVIRI clear-sky brightness temperature over sea for 3.9μm (red), 8.7μm (green), 10.8μm (blue), and 12.0μm (magenta) for July 2011**

This threshold is computed as:

$$T39thr = T39sim - 2.5\tau_s ErrOstia - 2\tau_s StdevCliOstia - Bias39 - Offset39$$

Where T39sim is the clear-sky brightess temperature simulated using local T_{Ostia} -0.2K as surface temperature, ErrOstia is the local error of T_{Ostia} , StdevCliOstia is the monthly climatology of Ostia standard deviation, Bias39 is the bias of the simulation, Offset39 a margin offset.

In order to be efficient and avoid cloud detection errors, the calculation of thresholds relying on clear-sky simulations must account for the bias between observations and simulations. A graph of their temporal variation for Meteosat-10 is given in. We can see that at least for IR 3.9 μm a near real-time monitoring should lead to change these mean biases, as the amplitude of the variation is about 0.6 K. With the experience of our ptototyping activity we recommand that the thresholds account for mean biases.

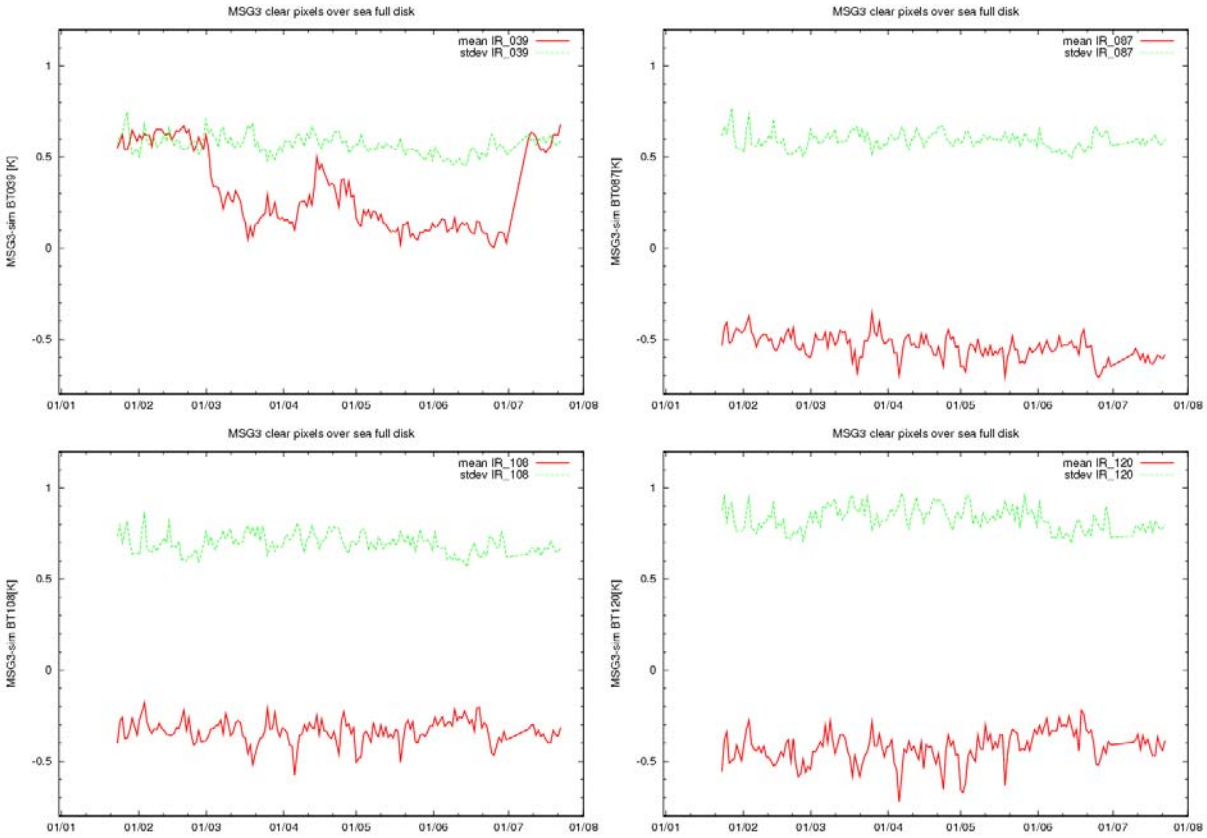

Figure 2 : **Mean and standard deviation of observed minus simulated SEVIRI brightness temperatures for clear pixels over sea at 00hUTC for 3.9μm (top left) , 8.7μm (top right) , 10.8μm (bottom left) and 12.0 μm (bottom right)**

Example of Namibian/Angolan boundary layer marine stratocumulus detection

During the third Cloud Retrieval Evaluation Workshop (CREW-3) meeting at Madison, USA, 15-18 November 2011, Gala Wind (NASA Goddard Space Flight Center) presented the results of her method to improve night-time low cloud detection over sea. She illustrated few cases where operational SAFNWC (V2009) cloud mask was missing some parts of the Namibian/Angolan marine stratocumulus at night. She designed, tested and illustrated a new correction algorithm using temporal image differencing of cloud pressure retrievals to locate cloud edges associated with uniform IR cloud top retrieval over ocean to improve the SAFNWC cloud mask.

In this example we applied only the direct thresholding of T3.9 with clear-sky RTTOV10 simulations using the 12h term ECMWF forecast from 10 August 2009 at 12h00 UTC (the 91 incoming hybrid levels are interpolated to the 51 RTTOV10 pressure levels by an internal RTTOV module). The surface temperature used in the simulation comes from OSTIA analysis on 9 August 2009. The following figure compares results presented by Gala Wind with the detections of our prototype threshold.

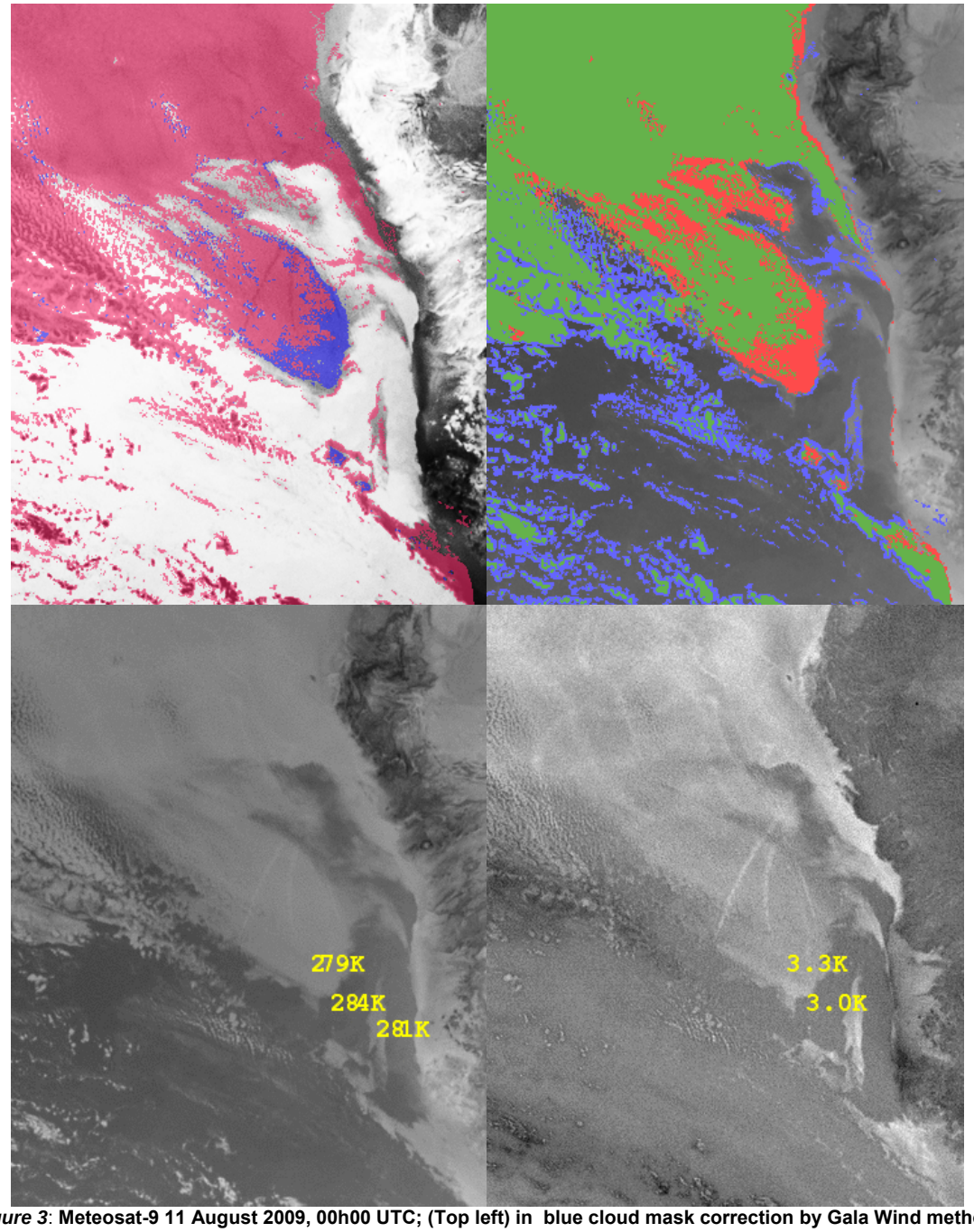

Figure 3: **Meteosat-9 11 August 2009, 00h00 UTC; (Top left) in blue cloud mask correction by Gala Wind method, SAFNWC cloud mask is pink; (Top right) in red cloud mask correction by thresholding T3.9, green corresponds to pixels detected both by prototype and operational SAFNWC, and blue are detections by other operational SAFNWC tests ; (Bottom left) T3.9, dark is warm, as in background of top right image; (Bottom right) T10.8-T3.9, clear grey corresponds to high values.**

Example of trade-wind low clouds detection

Trade-wind low clouds over sea are difficult to detect at night due to their small spatial and vertical extension. Such an example is illustrated below in the region of the Gulf of Aden and Arabian sea. On 5 March 2013, the offshore flow over the area is driven by the NorthEast monsoon season. A wide dry coastal zone along Oman and Yemen shore is terminated by a low and rather thin cloudy area appearing at night in the moist low atmosphere. This cloud layer is observed thanks to a low signature which can be seen in enhanced T10.8-T3.9 image. The behaviour of the prototype is rather satisfactory here as it improves the detection of the cloud without introducing false alarms.

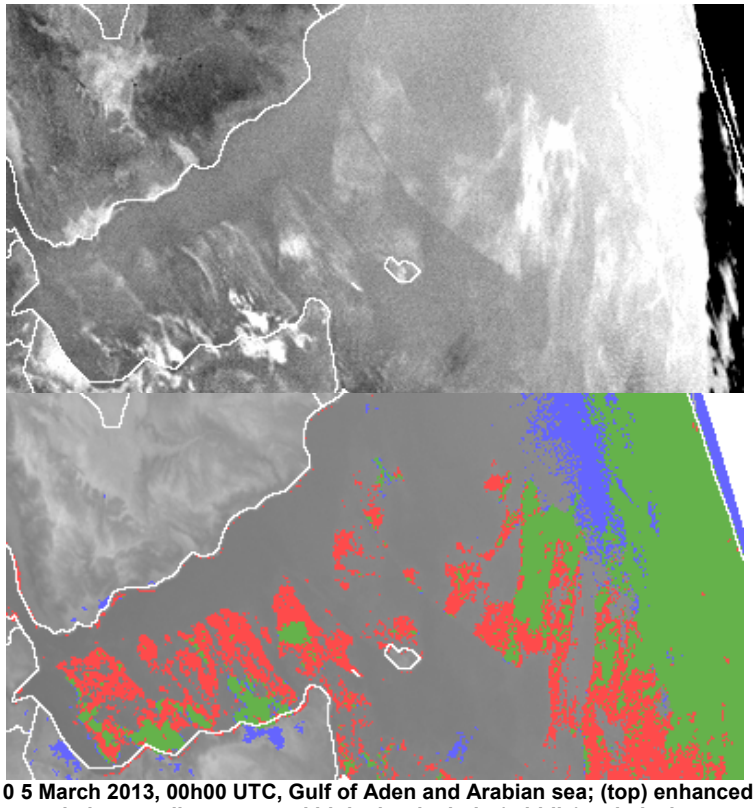

Figure 4 : **Meteosat-10 5 March 2013, 00h00 UTC, Gulf of Aden and Arabian sea; (top) enhanced T10.8-T3.9 with low clouds appearing clear, sea in intermediate gray and high clouds dark; (middle) red pixels correspond to correction of SAFNWC cloud mask with T39thr prototype, green corresponds to pixels detected both by prototype and operational SAFNWC, and blue are detections by other operational SAFNWC tests**

Cold water is not confused as cloud:example of Agulhas and Benguela currents junction

Off the Cape of Good Hope the cold north-flowing Benguela current (from Atlantic Ocean) and the warm south-flowing Agulhas current (from Indian Ocean) are mixing. Strong thermal fronts are observed here. An example of the behaviour of the prototype cloud mask in this area shows that cold coastal waters (5.5K colder than the warm vein of Agulhas current) are not confused as low clouds, while few low clouds are correctly added by the prototype.

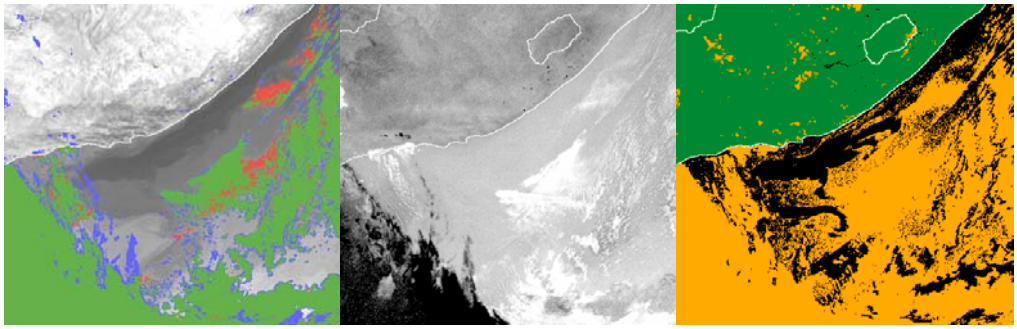

Figure 5 : **Meteosat-10 23 July 2013, 00h00 UTC ; (left) red pixels correspond to correction of SAFNWC cloud mask with T39 threshold prototype, green corresponds to pixels detected both by prototype and operational SAFNWC, and blue are detections by other operational SAFNWC tests, grey pixels are T10.8 (warm is dark); (middle) T10.8-T3.9 black low values and white (high values); (lright) MPEF cloud mask**

Detection of low clouds at night over barren grounds

The difference T8.7– 3.9 at night is useful to detect low clouds over barren grounds. Such surfaces have low (T8.7–T3.9) signatures (around 0K) whereas the low clouds exhibit high values. Therefore the contrast between the cloud and such a background is higher with (T8.7 – T3.9) than with (T10.8 –

T3.9). A threshold based on the comparison of RTTOV simulations and SEVIRI observations of (T8.7–T3.9) has been analysed. The following example illustrates its behaviour on a Sc deck being formed over the Atlantic Ocean and covering partially the Namib desert during the night-time cooling

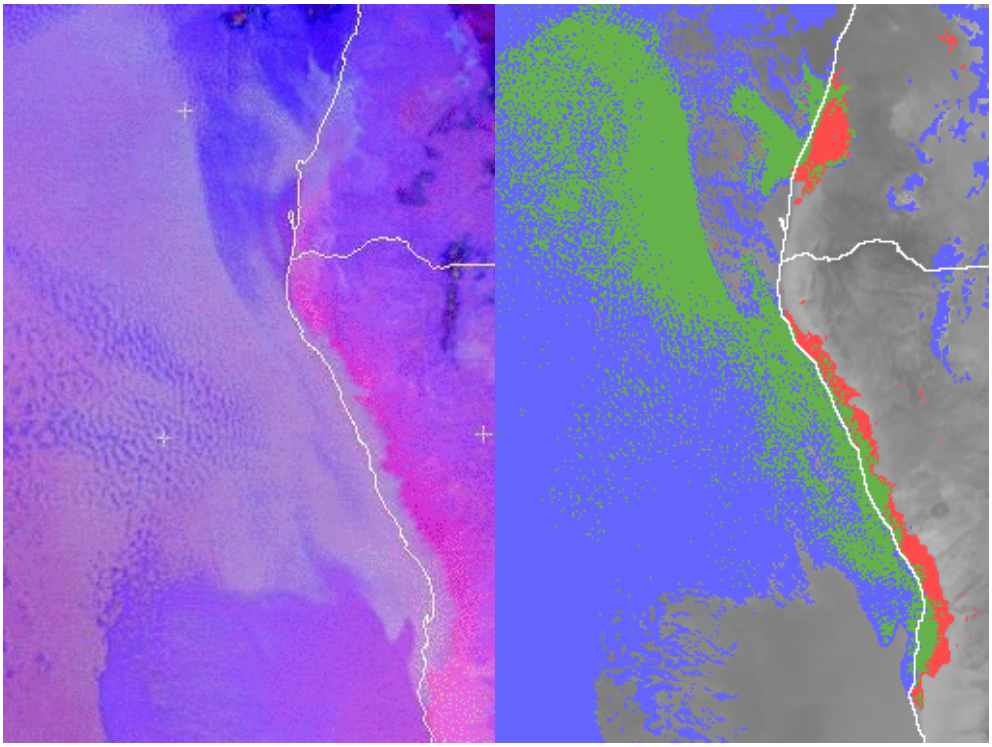

Figure 6 **: Meteosat-10, 2 March 2013 03h00UTC; EUMETSAT Fog RGB depicting low cloud spreading over Namib desert (left), Prototype T8.7-T3.9 direct thresholding (right), red pixels correspond to correction of SAFNWC cloud mask with prototype, green corresponds to pixels detected both by prototype and operational SAFNWC, and blue are detections by other operational SAFNWC test, grey pixels are T39 (warm is dark)**

Detection of low clouds over land in night-time in tropical conditions

The same (T8.7 – T3.9) threshold used to detect low clouds at night (sometimes it detects also dust clouds) over barren grounds is also efficient to detect clouds appearing at night in moist low layers of tropical atmosphere. Therefore it is used over land at night whatever the terrain type. An example observed by Meteosat-10 on 16 June 2013 over Cote d'Ivoire and Liberia illustrates its positive impact on the quality of the cloud mask. The heavy showers observed the previous day and the evaporation increased above vegetation at night favour the emergence of an abundant cloud cover. These clouds were only partially detected by the thresholds derived from look-up tables. The prototype T8.7 – T3.9 threshold derived from online RTTOV simulations improves their detection as shown below.

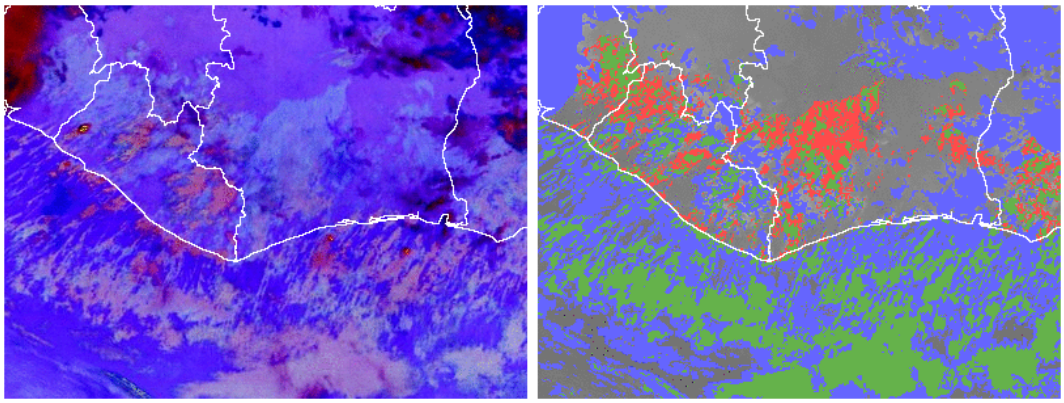

Figure 7 **: Meteosat-10 16 June 2013 03h00 UTC, Liberia and Cote d'Ivoire region; EUMETSAT Fog RGB (left); Prototype T8.7-T3.9 direct thresholding (right), red pixels correspond to correction of SAFNWC cloud mask**

Dust clouds over barren ground in night-time

It happens that (T8.7 – T3.9) threshold detects also dust clouds. The following figure illustrates the behaviour of the prototype (T8.7 – T3.9) threshold for such an event observed .

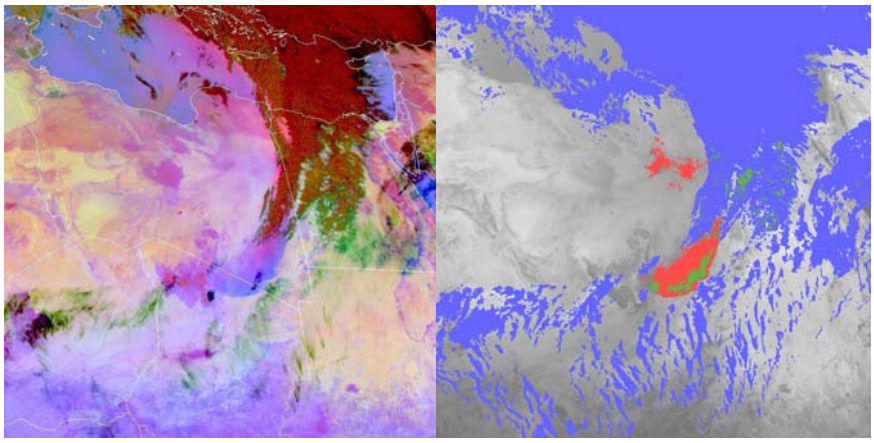

Figure 8 : **Meteosat-10, 22 February 2013 00h00 UTC ; EUM dust RGB (left) Prototype T8.7-T3.9 direct thresholding (right), red pixels correspond to correction of SAFNWC cloud mask with prototype**

Low clouds over ground with high viewing angles

Current NWCSAF cloud mask makes use of T10.8 – T8.7 at high satellite angles to improve the detection of low clouds (T10.8-T3.9 becomes less efficient when viewing angle is high). We have prototyped a direct thresholding of T10.8 – T8.7 and observed its behaviour. Its impact on a poor detection by operational SAFNWC cloud mask is illustrated below. The red pixels added by the prototype are more numerous when viewing angle increases. Only very few false alarms appear over Caucasu mountains between Black Sea and Caspian Sea, at the border between Georgia and Russian federation. To avoid these false alarms the final test will not be applied over mountains.

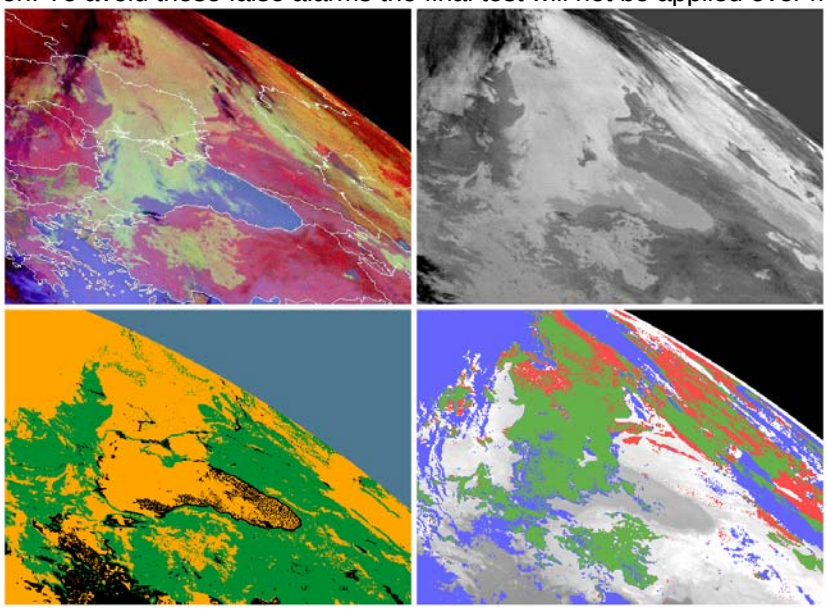

Figure 9 : **Meteosat-9 3 January 2013 00h00 UTC; Fog RGB (top left); T10.8-T8.7 clear gray pixels are low clouds (top right);MPEF Cloud mask (bottom left); Prototype T10.8-T8.7 direct thresholding (bottom right), red pixels correspond to correction of SAFNWC cloud mask with prototype**

CONCLUSION

Prototyping activity has clearly shown that in-line clear-sky simulations improve the quality of NWCSAF GEO Cloud mask particularly in night-time. It appeared also that the threshold efficiency may depend on the temporal evolution of the mean biases between simulations and observations. These biases are sensitive to changes related to instrument calibration (for instance decontamination periods for SEVIRI 3.9μm of Meteosat-10) but also to the NWP environment. Therefore NWCSAF GEO v2015 will be delivered with biases by default adapted to ECMWF. These biases must be monitored.
The users of the NWCSAF GEO software relying on their own NWP must monitor their biases and replace the default values of the standard installation by their values. We keep the current look-up table approach, much less NWP sensitive, and add the in-line clear-sky simulations as an option. Of course we incline the users towards enabling it when possible, and we expect our paper inciting, before NWCSAF GEO Cloud mask 2015 full validation.

REFERENCES

Derrien M. and Le Gléau, 2005: MSG/SEVIRI Cloud Mask and Type from SAFNWC, International Journal Of Remote Sensing, 21, 4707-4732, DOI: 10.1080/01431160500166128

Derrien M. and Le Gléau H., 2010: Improvement of cloud detection near sunrise and sunset by temporal-differencing and region-growing techniques with real-time SEVIRI. *International Journal of Remote Sensing,* **31**,7 1765-1780, DOI: 10.1080/01431160902926632

Derrien M., Le Gléau H., Raoul M.P., 2010 The use of the high resolution visible in SAFNWC/MSG Cloud Mask. 2010, EUMETSAT Meteorological Satellite Conference, Cordoba, Spain, 20-24 September 2010

Heidinger A., 2011, Algorithm Theoretical Basis Document ABI Cloud Mask, Version 2, accessed at http://www.goes-r.gov.

Hocking J., Francis P.N., Saunders R., 2011, Cloud detection in Meteosat Second Generation at the Met Office. Meteorol.Appl. **18**: 307-323 DOI: 10.1002/met.239

Lutz H.J., König M., 2008, The use of Surface Emissvity Information within the Meteosat Second Generation Meteorological Product Generation. The 2008 EUMETSAT Conference, Darmstadt, Germany, 8-12 September 2008

John D. Stark, Craig J. Donlon, Matthew J. Martin and Michael E. McCulloch, 2007, *OSTIA : An operational, high resolution, real time, global sea surface temperature analysis system.*, Oceans '07 IEEE Aberdeen, conference proceedings. Marine challenges: coastline to deep sea. Aberdeen, Scotland.

Wind G., 2011, Improvements in night-time low cloud detection and MODIS-style cloud optical properties from MSG-SEVIRI. Third Cloud Retrieval Evaluation Workshop (CREW-3) 15-18 November 2011, USA, Madison